Research Article

A facile synthesis of implantation of silver nanoparticles on oxygen-functionalized multi-walled carbon nanotubes: structural and antibacterial activity

Pavani Tambur[1] · D. Bhagawan[1] · B. Siva Kumari[3] · Ramamohan Reddy Kasa[2]

Received: 29 January 2020 / Accepted: 18 April 2020 / Published online: 28 April 2020

Abstract
Silver nanoparticles imply as a promising competitor for enhancement of future antibacterial treatments due to its wide range of activity. The present study reports the implantation of Oxygen-functionalized Multi-Walled Carbon Nanotubes (O-MWCNTs) onto Silver nanoparticles in their pure phase are warily and homogenously implanted via facile approach by means of silver nitrate as precursor material. X-ray Diffraction was performed to detect crystalline size; differentiation of bands for P-MWCNTs, O-MWCNTs and Ag-MWCNTs was detected by Fourier Transform Infrared Spectroscopy; the exact shift was clearly depicted using Raman Spectroscopy; weight loss percentage through Thermogravimetric Analysis; potential values by Zeta Potential; Size, morphology and elemental analysis using Transmission Electron Microscopy and FE-SEM with EDX respectively. The antibacterial studies of Ag-MWCNTs were performed for four bacterial strains i.e., *Bacillus subtilis, Staphylococcus aureus*, *Escherichia coli* and *Pseudomonas aeruginosa* through disc diffusion method. As the concentration of Ag-MWCNTs was high, the zone of inhibition is high especially in Gram+ve bacteria signifying as a good anti-bacterial agent.

✉ Ramamohan Reddy Kasa, kasarammohan@gmail.com | [1]Centre for Environment, Institute of Science and Technology, JNTUH, Hyderabad, India. [2]Centre for Water Resources, Institute of Science and Technology, JNTUH, Hyderabad, India. [3]Department of Botany, Andhra Loyola College, Vijayawada, India.

SN Applied Sciences (2020) 2:981 | https://doi.org/10.1007/s42452-020-2797-x

Graphic abstract

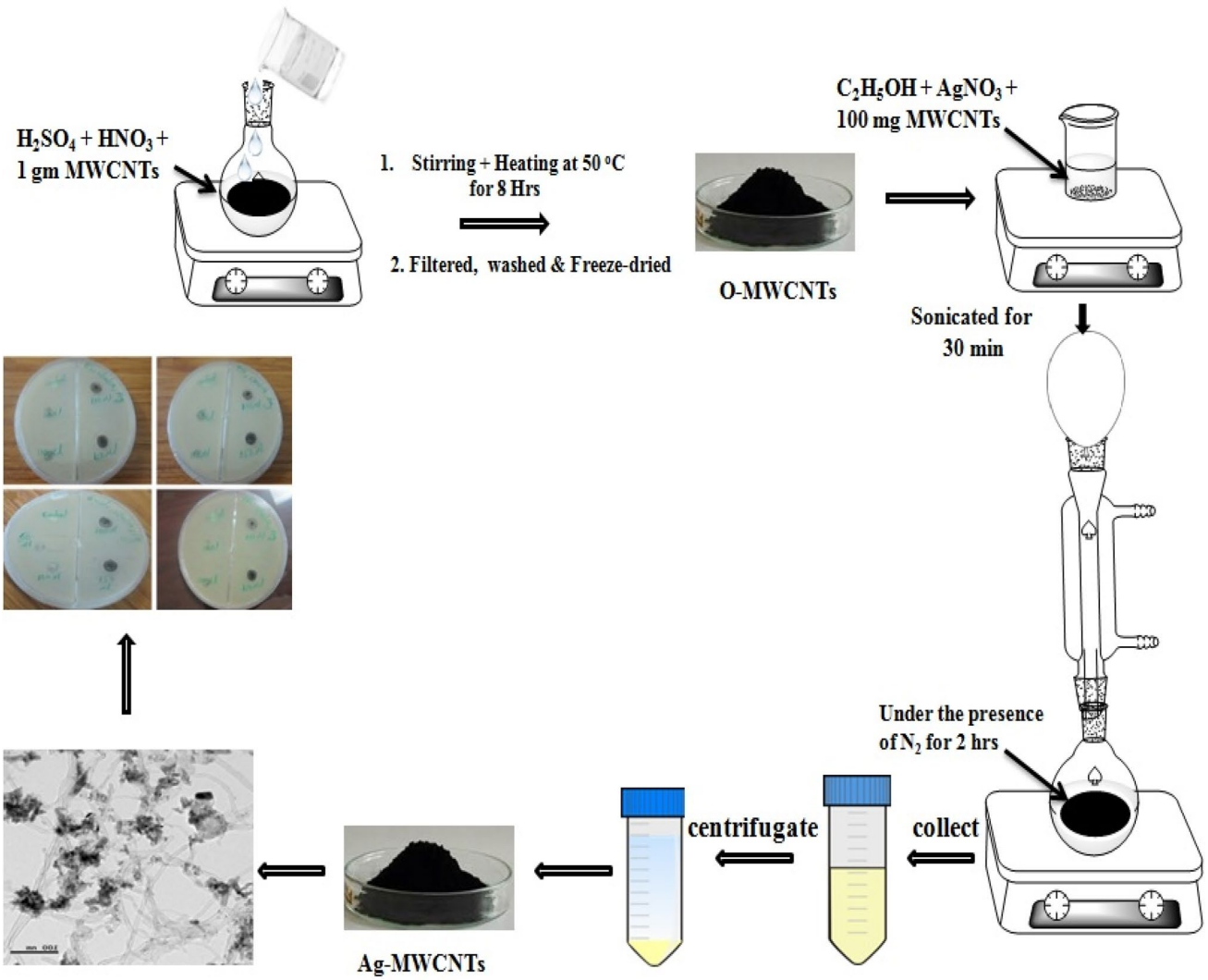

Keywords Ag-MWCNTs · Raman spectroscopy · X-ray diffraction (XRD) · Transmission electron microscopy (TEM) · FE-SEM with EDX · Antibacterial study

1 Introduction

Multi walled carbon nanotubes (MWCNTs) comprise an encouraging application in almost all aspects of Nanotechnology [1]. In contrast to other material forms of carbon–diamond and graphite, carbon nanotubes (CNTs) are one dimensional and support to function specifically in preparing metal, metal oxide CNT composites [2, 3]. In recent times, silver nanoparticles decorated on MWCNTs as composite material has attracted significant interest with abundant array of latent applications in the field of solar power alteration and photo catalysis [4, 5]. It is well known that the binding of metal nanoparticles on to the surface of CNTs (CNTs-Metals) is very poor [6]. It has been reported [7] by the inclusion of defects and functional groups on CNTs, the surface reactivity can be increased. Therefore, functional groups like carboxyl (–COOH), carbonyl (–C=O) and hydroxyl (–OH) are created by treating CNTs with strong acids [8] that would enhance their properties. Acid treatment leads to interfacial bonding between the metal atoms, defective and oxidized CNTs to make certain tremendous mechanical performances for the CNT-reinforced metal-matrix composites.

The significance of bactericidal nanomaterials is due to the amplified resistant strains of bacteria against most potent antibiotics and has promoted the research in the

antibacterial properties of nanoparticles. In the present paper, the synthesis of Ag nanoparticles decorated MWCNTs (Ag-MWCNTs) by reduction process and characterized by various characterization techniques is reported. Antibacterial activities against two Gram negative bacteria and two Gram-positive bacteria have been studied. A similar antimicrobial activity study using various other nanoparticles is reported in literature [9].

Bacillus subtilis is a rod shaped Gram-positive microorganism, catalase-positive bacterium also recognized as Vibrio subtilis, hay or grass bacillus. It is considered as model organism for laboratory analysis. *Staphylococcus aureus* is a round shaped Gram-positive bacterium originates majorly inside upper respiratory tract and on skin. *Escherichia coli* are rod-shaped, coliform Gram-negative bacteria. Analogous to *B. subtilis*, *E. coli* is considered as model organism in microbiology studies. *Pseudomonas aeruginosa* is a rod-shaped Gram-negative bacterium. It has special importance in medical field as multidrug resistant pathogen.

2 Experimental methods

2.1 Acid treatment of MWCNTs

Surface treatment of pristine (P-MWCNTs) with a combination of concentrated H_2SO_4 and HNO_3 in a molar ratio of 3:1 were result in generate Oxygen functionalities. Under invariable stirring at 50 °C for 8 h, 75 ml of H_2SO_4 (97%) and 25 ml of concentrated HNO3 (65%) were carefully varied together and added to 1 g of (P-MWCNTs) and was heated in a round bottom flask. Equal quantity of deionized water was added and then filtered after cooling to room temperature. The residue was filtered and freeze-dried until neutral pH was attained and washed several times with deionised water. [10, 11] Oxidized Multi Walled Carbon Nanotubes will be henceforth termed as O-MWCNTs.

2.2 Decoration of silver nanoparticles on O-MWCNTs

50 ml ethanol and 77.2 mg of silver nitrate (15 wt % of Ag) was suspended in 30 ml of ethanol independently and then 100 mg of O-MWCNTs was dispersed and sonicated for 30 min before blending both the solutions. At this point a nitrogen stream of 50 ml min^{-1} was raised through the slurry to cleanse broke down oxygen and to accomplish a dormant response climate. The bunch reactor was illuminated for 4 h utilizing a LuzChem photoreactor furnished with 14 low pressure mercury lights (8 W, $\lambda_{max} = 360$ nm). After the light time, the acquired material was washed with ethanol, isolated by centrifugation and it was dried at 50 °C in a show stove. After centrifugation, the centrifugate was washed with deionized water and dried at 200 °C under the progression of nitrogen at a pace of 300 µl per min for 2 h.

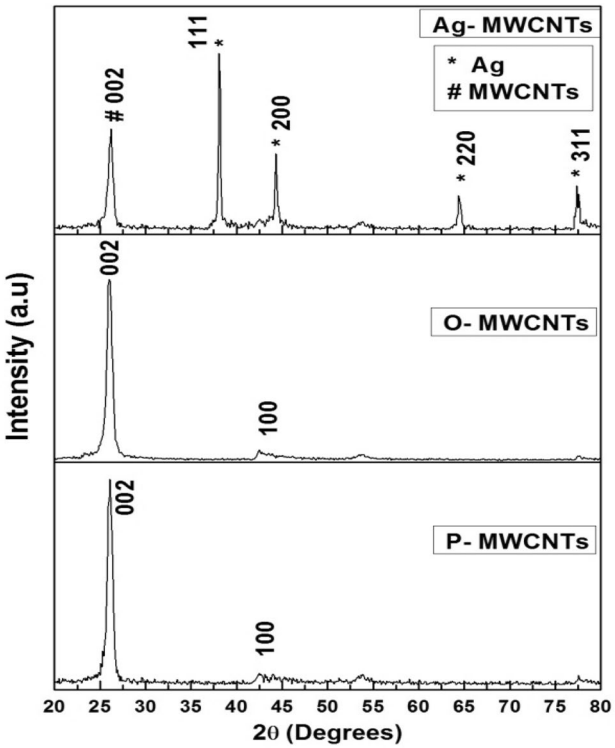

Fig. 1 XRD patterns of P-MWCNTs, O-MWCNTs, Ag-MWCNTs

2.3 Disc diffusion method

Kirby-Bauer Disc diffusion technique was employed to analyse the antimicrobial activity of Ag-MWCNTs. Materials used for antibacterial activity of Ag-MWCNTs include Nutrient broth 1.3 g, Agar–agar 1.5 g, petriplates, cotton swabs, *B. subtilis (ATCC 6633), S. aureus (ATCC 25923), E. coli(ATCC 25922)*and *P. aeruginosa (ATCC 27853)*.

In four conical flasks, nutrient broth (1.3 g in 100 ml D/W) was arranged and sterilized. In two conical flasks, clinically isolated strain of *B. subtilis* and *S. aureus* were inoculated respectively and in the other two conical flasks clinically isolated strain of *E. coli and P. aeruginosa* were added. The bacterial culture inoculated nutrient broth was kept on rotary shaker for 24 h at 100 r.p.m. On the entire surface of the plates, four pathogenic strains *B. subtilis, S. aureus, E. coli* and *P. aeruginosa* were taken and spread evenly. The plates were allowed to dry completely and then sample was applied. 500 µl of nutrient broth culture of each bacterial organism was added to 100 ml solution of various concentrations of Ag-MWCNTs ranging from 50 to

200 mg/µl. All the test plates were wrapped with parafilm tape and kept in incubator for 24 h at 37 °C [12].

3 Results and discussions

3.1 XRD

Using X-ray diffraction (XRD) the structure furthermore dimensions of MWCNTs were studied and shown in the Fig. 1. The two diffraction peaks at 2θ = 26° and 43° correspond to *hkl* reflections (002) and (100) for Pristine-MWCNTs and O-MWCNTs signifying that MWCNTs were intact still after acid treatment [13]. The ardent examination in XRD figure represents the modification of MWCNTs as the graph was smooth and the shift of the peaks was very small in O-MWCNTs. By the reduction of Ag ions in ethanol, silver nanoparticles were successively impregnated on the functional groups of the MWCNTs [14]. The (002) plane with diffraction peak could be related to MWCNT and the other peaks detected at 2θ = 37.80°, 44.3°, 64.46°, and 77.36° correlate to the (111), (200), (220), and (311) planes respectively that was matching with #04-0783 JCPDS Card, indicating the regular peaks for silver with face-centered structure [15]. Debye–scherrer equation was used to determine the crystalline size of the particles [16] Ag-MWCNTs have crystalline size of 30 nm.

$$\mathcal{D} = \frac{0.9\lambda}{\beta cos\theta} \tag{1}$$

where λ is X-ray wavelength (1.54 Å), β is the full width at half maximum (FWHM) of the diffraction peak and θ is the Bragg's diffraction angle respectively.

The cumulative dislocation density was indicated at 1.1×10^{16} Lines/m^2. Crystalline size is important parameter to calculate Dislocation density (δ).

$$\delta = \frac{1}{\mathcal{D}^2} \tag{2}$$

Micro strain was calculated by the subsequent formula given below. Due to the lattice misfit, micro strain arises and varies on the deposition conditions as a regulating factor. The collective micro strain was 1.29×10^{-3} Lines^{-2}/m^4.

$$\varepsilon = \frac{(\beta \cos\theta)}{4} \tag{3}$$

3.2 Fourier transform-infrared spectroscopy (FT-IR) analysis

Fourier transformed infrared spectroscopy spectrum was plotted against transmittance versus wave number (cm^{-1}) with a range about 500–4000 cm^{-1} for P-MWCNTs, O-MWCNTs and Ag-MWCNTs as indicated in Fig. 2. P-MWCNTs, O-MWCNTs and Ag-MWCNTs with abroad peak at 3423.43 cm^{-1}, 3443.78 cm^{-1}and 3442.87 cm^{-1}are attributed to the OH stretching mode for all the three samples respectively [17]. Due to oxidation on MWCNTs surface, Carbonyl group at 1695.38 cm^{-1}and 1695.98 cm^{-1} were observed. For O-MWCNTs the C=C stretching band assigned at 1602.06 cm^{-1}and methylene group (CH_2) stretching bands at 2885.63 cm^{-1}. COOH group was observed at 1720.56 cm^{-1}. Ag–C stretching mode was observed at 609.49 cm^{-1} [18].

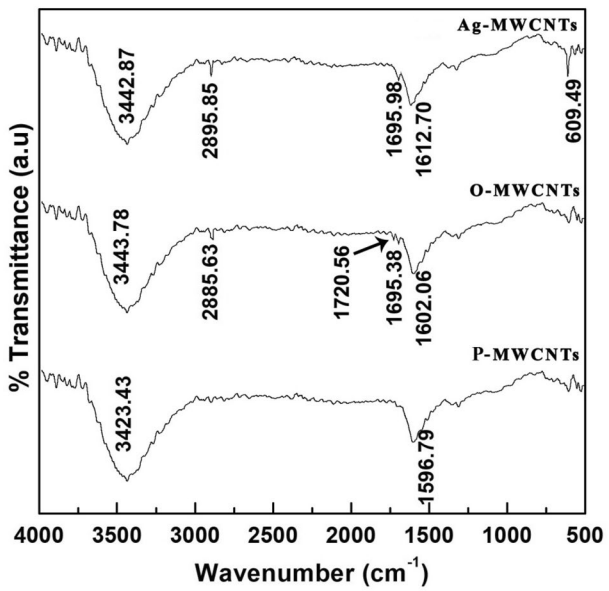

Fig. 2 FT-IR spectra of P-MWCNTs, O-MWCNTs, Ag-MWCNTs

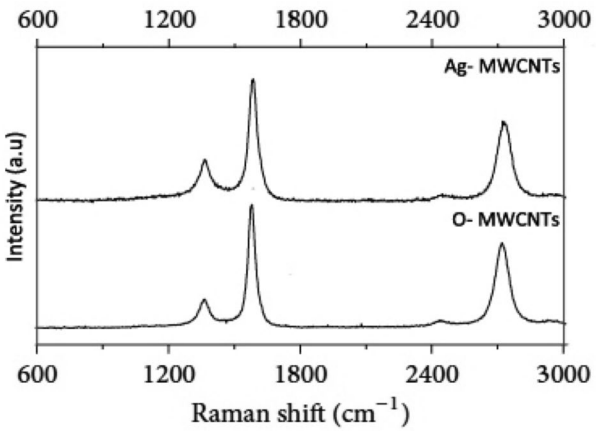

Fig. 3 Raman spectroscopy of O-MWCNTs and Ag-MWCNTs

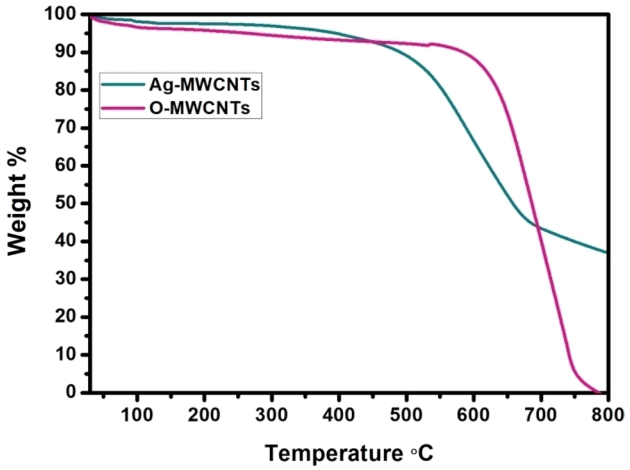

Fig. 4 TGA curves of O-MWCNTs and Ag-MWCNTs

3.3 Raman spectroscopy

As shown in Fig. 3 Raman spectroscopy is an effective tool to characterize any material in general and doped materials. For O-MWCNTs and Ag-MWCNTs Raman Spectra range from the wave number 600–3000 cm^{-1}. Due to carbon–carbon bond stretching in the graphite plane and defects/impurities in the MWCNTs peaks of O-MWCNTs for D′band at 1350 $cm^{-1}$and G′band at 1576 cm^{-1} was observed. For Ag-MWCNTs, D′band is shifted to 1352 cm^{-1} and G-band is shifted to 1578 cm^{-1} representing the change in-plane lattice constant and a weakening of either Ag–C or C–C in plane bond strengths relative to that of a C–C bond. A second order G′ band was evident at 2750 cm^{-1} and 2751 cm^{-1} for both O-MWCNTs and Ag-MWCNTs respectively. The G′ peak for Ag-MWCNT shifted to a higher wave number 2751 cm^{-1} because of charge shift interface among the Ag nanoparticles and MWCNTs. Intensity ratio values of D′ and G′ bands for O-MWCNTs and Ag-MWCNTs were 0.24 and 0.39 respectively, speculating raise in the degree of disorder of the MWCNT walls following the inclusion of Silver nanoparticles [19].

3.4 Thermogravimetric analysis

Temperature (°C) versus Weight loss (%) graph was drawn to represent thermogravimetric analysis Fig. 4. At 800 °C, O-MWCNTs weight was 89.4%, and due to disintegration of –OH groups and –COOH groups, 10.6% weight loss was observed. The weight of Ag-MWCNTs remained 79.20% at 800 °C and 20.8% weight loss.

3.5 Zeta potential

Particle Size Analyzer was used to know zeta potential of Ag-MWCNTs. These silver-MWCNTs are diffused in ethanol and tested. The results were shown in the Figs. 5, 6 and 7 i.e., P-MWCNTs, O-MWCNTs and Ag-MWCNTs. Zeta potential of O-MWCNTs in ethanol decreased from − 8.8 to − 18.2 mV after the acid treatment. Due to acid treatment negatively charged groups are introduced on MWCNTs [20]. By decoration of silver on MWCNTs, the zeta potential of composite become more positive than non-functionalised MWCNTs and O-MWCNTs. It could be understood that negative charge on MWCNTs is reduced by the deposition of metal and metal oxides [21, 22].

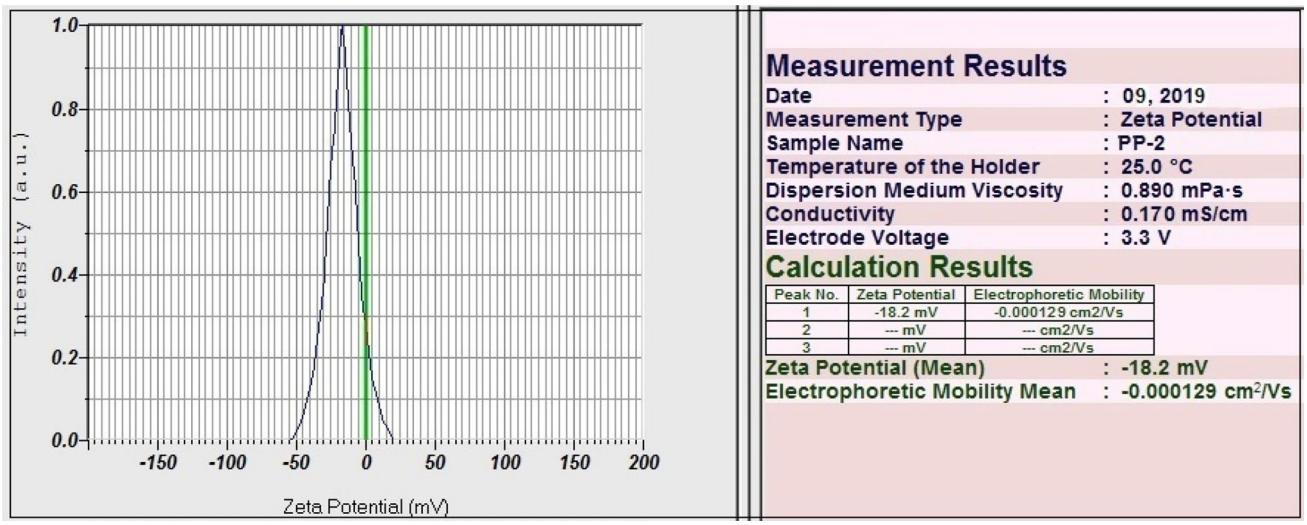

Fig. 5 Zeta potential of P-MWCNTs

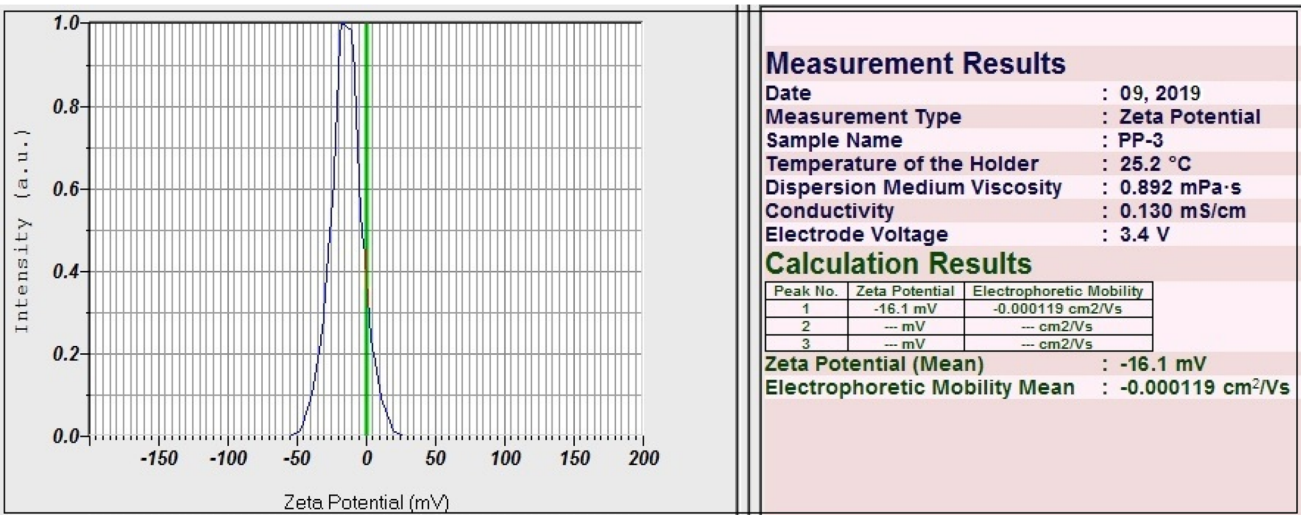

Fig. 6 Zeta potential of O-MWCNTs

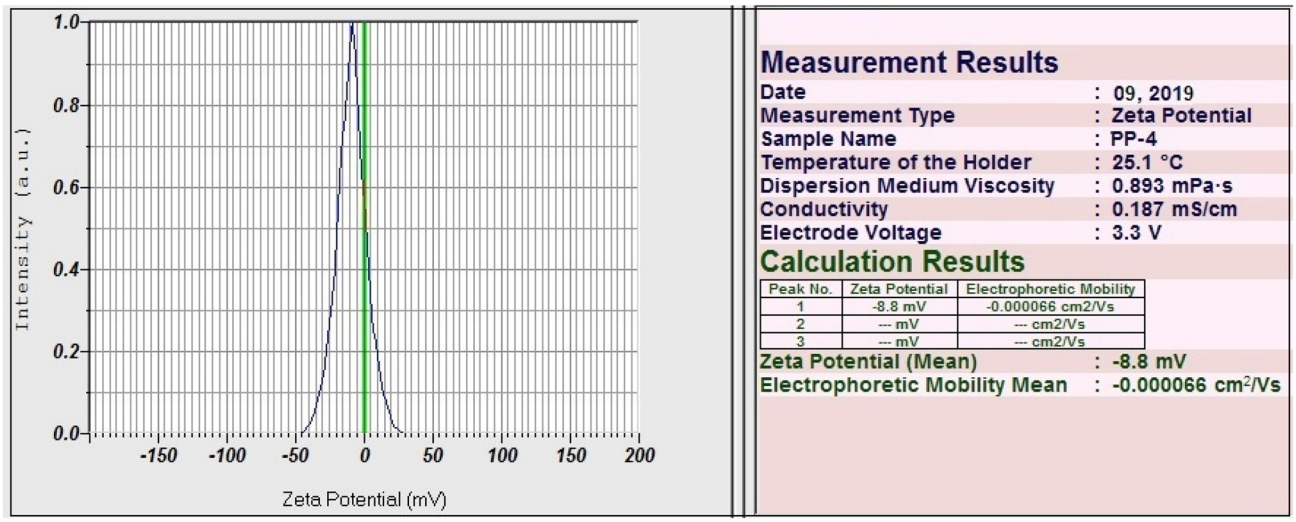

Fig. 7 Zeta potential of Ag-MWCNTs

3.6 Transmission electron microscope (TEM)

Figure 8 represents the morphology of the Silver -treated MWCNTs by TEM. Silver nanocrystals are in irregular shapes and dispersed on MWCNTs surface. At 100 nm magnification, the TEM result ranges between 20 and 60 nm for silver containing nanoparticles. Due to capillary action of small particles, they are well distributed all over the surface collectively and formed a slightly large mass with compact shape and conglomerated [23]. During the acid treatment, MWCNTs might have broken but importantly functional groups were added on MWCNTs.

3.7 Field emission scanning electron microscope (FESEM) with energy dispersive X-ray spectrometer (EDX)

The synthesized Ag-MWCNTs micrograph Fig. 9a, b indicate the presence of spiral, thread shape cubic and few irregular granulated compact agglomerates. EDX report Fig. 9c, d signify the chemical composition/contaminants present in the synthesized sample; indicating carbon, silver and elemental oxygen peaks with the elemental composition weight % of 75.4 Carbon, 23.9% Silver, 0.7% Oxygen.

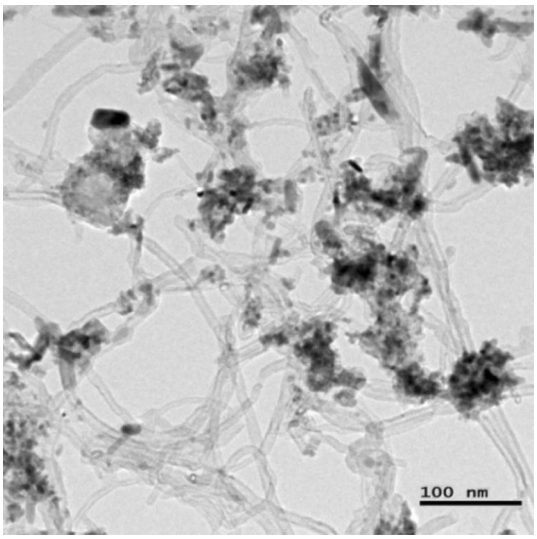

Fig. 8 TEM micrograph of Ag-MWCNTs

3.8 Antibacterial activity

Inhibition zones confirmed antibacterial activity of Ag-MWCNTs. The present study was focussed on CNTs and its composites for antibacterial activity. There were studies indicating that electrical properties were associated with antibacterial activity [24]. Silver nanoparticles decorated on MWCNTs were tested for antibacterial activity against Gram-Positive *B. subtilis* and *S. aureus* and *E. coli* and *P. aeruginosa* Gram-Negative bacteria. At 37 °C for 24 h, the *B. subtilis*, *S. aureus*, *E. coli* and *P. aeruginosa* incubated after treating with Ag-MWCNTs concentrations ranging from 50 to 200 µl at 50 µl interval exposed Fig. 10a, b, c and d. It was observed that gram positive bacteria were effective as gram negative bacteria as zone of inhibition was high in former one. The zone of inhibition values were indicated in Table 1 *B. subtilis* and *S. aureus are* Gram positive bacteria and have a thick cell wall containing numerous

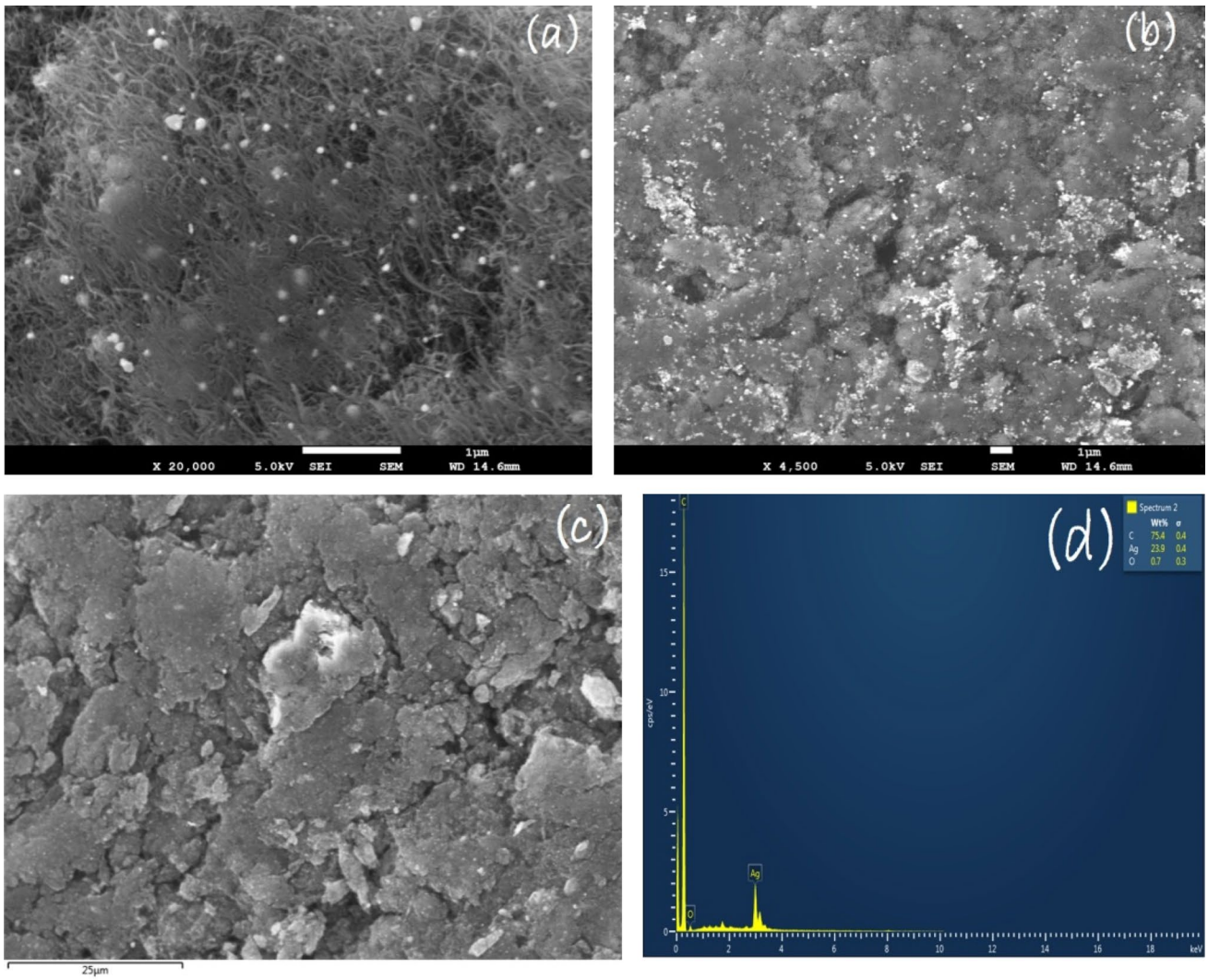

Fig. 9 FESEM and EDAS images of Ag-MWCNTs

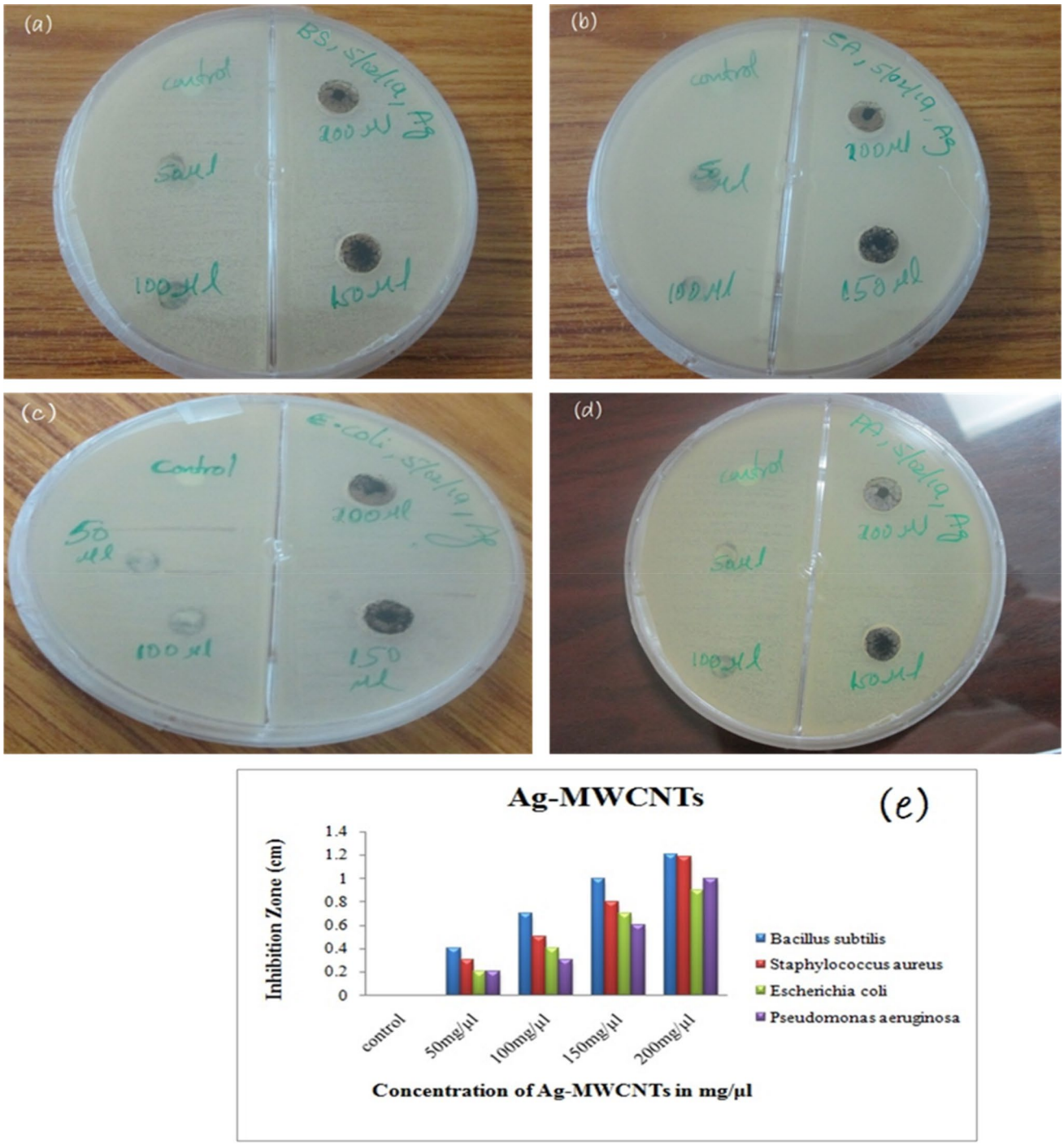

Fig. 10 Antibacterial activity of Ag- MWCNTs on **a** *B. subtilis*, **b** *S. aureus*, **c** *E. coli*, **d** *P. aeruginosa*, **e** Zone of inhibition (cm) shown by Ag-MWCNTs at different concentrations

mucopeptides, murein and lipoteichoic acids. The outer membrane walls of bacteria might be damaged by the reactive radicals like O^{2-}, –OH and H_2O_2 [25, 26]. It is also known that when MWCNTs are in direct contact with cell, they could damage the Cellular membrane's integrity, surface and metabolic activity of *B. subtilis*, *S. aureus*, *E. coli* and *P. aeruginosa*. Thus, MWCNTs damage the cell membrane and oxidative states endure the stress [27]. Figure 3e signifies the antibacterial results. Related results were observed for Fe_3O_4 and copper nanoparticles on the antibacterial activity of 4 bacterial strains [28].

Table 1 Representation of inhibition zone (cm)

S. no.	Ag-MWCNTs concentration	Test organisms inhibition zone in (cm)			
		B. subtilis Gram+ve	*S. aureus* Gram+ve	*E. coli* Gram−ve	*P. aeruginosa* Gram−ve
1	Control	0	0	0	0
2	50 mg/µl	0.4	0.3	0.2	0.2
3	100 mg/µl	0.7	0.5	0.4	0.3
4	150 mg/µl	1.0	0.8	0.7	0.6
5	200 mg/µl	1.2	1.18	0.9	1.0

4 Conclusions

The silver nanoparticles are decorated successfully on functionalised MWCNTs. In the present study it was indicated from XRD, Raman Spectroscopy and TEM results that functionalised MWCNTs could be a good support for silver nanoparticles. The size, dislocation density and micro stains of the silver nanoparticles are evaluated. The dislocation density was 1.1×10^{16} Lines/m^2. Similarly, the micro strain was 1.29×10^{-3} Lines^{-2}/m^4. Raman spectroscopy revealed that MWCNTs were not distorted and silver nanoparticles were successfully decorated. The Zone of inhibition confirmed the antibacterial activity of Ag-MWCNTs. It was concluded that Ag-MWCNTs are very effective antibacterial agent.

Compliance with ethical standards

Conflict of interest The authors declare that they have no conflict of interest.

References

1. Iijima S (1991) Helical microtubules of graphitic carbon. Nature 354:56–58
2. Wildgoose GG, Banks CE, Compton RG (2006) Metal nanoparticles and related materials supported on carbon nanotubes: methods and applications. Small 2:182–193
3. Georgakilas V, Gournis D, Tzitzios V, Pasquato L, Guldi DM, Prato M (2007) Decorating carbon nanotubes with metal or semiconductor nanoparticles. J Mater Chem 17:2679–2694
4. Robel I, Bunker BA, Kamat PV (2005) Single-walled carbon nanotube–CdS nanocomposites as light-harvesting assemblies: photoinduced charge-transfer interactions. Adv Mater 17:2458–2463
5. Jiang LQ, Gao L (2005) Fabrication and characterization of ZnO-coated multi-walled carbon nanotubes with enhanced photocatalytic activity. Mater Chem Phys 91:313–316
6. Ayala P, Freire FL Jr, Gu L, Smith DJ, Solrzano IG, Macedo DW, Sande VJB, Terrones H, Rodriguez-Manzo J, Terrones M (2006) Decorating carbon nanotubes with nanostructured nickel particles via chemical methods. Chem Phys Lett 431:104–109
7. Fan Q-Q, Qin Z-Y, Liang X, Li L, W-H Wu, Zhu M-F (2010) Reducing defects on multi-walled carbon nanotube surfaces induced by low-power ultrasonic-assisted hydrochloric acid treatment. J Exp Nanosci 5:337–347
8. Kundu S, Wang Y, Xia W, Muhler M (2008) Thermal stability and reducibility of oxygen-containing functional groups on multiwalled carbon nanotube surfaces: a quantitative high-resolution XPS and TPD/TPR study. J Phys Chem C 112:16869–16878
9. Khan MM, Ansari SA, Lee J-H, Ansari MO, Lee J, Cho MH (2014) Electrochemically active biofilm assisted synthesis of Ag@ CeO2 nanocomposites for antimicrobial activity, photocatalysis and photoelectrodes. J Colloid Interface Sci 431:255–263
10. Jesus JC, González I, Quevedo A, Puerta T (2005) Thermal decomposition of nickel acetate tetrahydrate: an integrated study by TGA, QMS and XPS techniques. J Mol Catal A Chem 228:283–291
11. Lin KY, Tsai WT, Chang JK (2010) Decorating carbon nanotubes with Ni particles using an electroless deposition technique for hydrogen storage applications. Int J Hydrog Energy 35:7555–7562
12. Prabhu YT, Rao KV, Kumari BS, Pavani T (2015) Decoration of magnesium oxide nanoparticles on O-MWCNTs and its antibacterial studies. Rend Fis Acc Lincei 26:263–270
13. Liu F, Zhang XB, Haussler D, Jager W, Yi GF, Cheng JP, Tao XY, Luo ZQ, Zhou SM (2006) TEM characterization of metal and metal oxide particles supported by multi-wall carbon nanotubes. J Mater Sci 41:4523–4531
14. Gupta S, Farmer J (2011) Multiwalled carbon nanotubes and dispersed nanodiamond novel hybrids: Microscopic structure evolution, physical properties, and radiation resilience. J Appl Phys 109:014314–014315
15. Yuan W, Jiang G, Che J et al (2008) Deposition of silver nanoparticles on multiwalled carbon nanotubes grafted with hyperbranched poly (amidoamine) and their antimicrobial effects. J Phys Chem C Nanomater Interfaces 112:18754–18759
16. Pal J, Chauhan P (2009) Structural and optical characterization of tin dioxide nanoparticles prepared by a surfactant mediated method. Mate Charact 60:1512–1516
17. Titus E, Ali N, Cabral G, Gracio J, Babu PR, Jackson MJ (2006) Chemically functionalized carbon nanotubes and their characterization using thermogravimetric analysis, fourier transform infrared, and raman spectroscopy. J Mater Eng Performance 15:182–186
18. Javad S, Soheila GR (2014) Silver decorated multi-walled carbon nanotubes as a heterogeneous catalyst in the sonication of 2-aryl-2,3-dihydroquinazolin-4(1H)-ones. RSC Adv 4:11654
19. Pimenta MA, Dresselhaus G, Dresselhaus MS, Cancado LG, Jorio A, Saito R (2007) Studying disorder in graphite-based systems by Raman spectroscopy. Phys Chem Chem Phys 9:1276–1291
20. Koch S, Woias P, Meixner LK, Drost S, Wolf H (1999) Protein detection with a novel ISFET-based zeta potential analyzer. Biosens Bioelectron 14:413–421
21. de la Cruz EF, Zheng Y, Torres E, Li W, Song W, Burugapalli K (2012) Zeta potential of modified multi-walled carbon nanotubes in presence of poly (vinyl alcohol) hydrogel. Int J Electrochem Sci 7:3577–3590
22. Gonzalez-Campos JB, Mota-Morales JD, Kumar S, Zarate-Trivino D, Hernandez-Iturriaga M, Prokhorov E, Vazquez-Lepe M, García-Carvajal ZY, Sanchez IC, Luna-Barcenas G (2013) New insights into the bactericidal activity of chitosan-Ag bionanocomposite: the role of the electrical conductivity. Colloid Surf B Biointerface 111:741–746
23. Longshan X, Xiaohua C, Weiying P, Wenhua L, Zhi Y, Yuxing P (2007) Electrostatic-assembly carbon nanotube-implanted copper composite spheres. Nanotechnology 18(43):435607

24. Boudreau MA, Fisher JF, Mobashery S (2012) Messenger functions of the bacterial cell wall-derived muropeptides. Biochemistry 51(14):2974–2990
25. Padmavathy N, Vijayaraghavan R (2008) Enhanced bioactivity of ZnO nanoparticles—an antimicrobial study. Sci Technol Adv Mater 9:035004
26. Zhu XY, Bai RB, Wee KH, Liu CK, Tang SL (2010) Membrane surfaces immobilized with ionic or reduced silver and their antibiofouling performances. J Membr Sci 363:278–286
27. Prabhu YT, Rao KV, Kumari BS, Kumar VSS, Tambur P (2015) Synthesis of Fe_3O_4 nanoparticles and its antibacterial application. Int Nano Lett 5:85–92
28. Prabhu YT, Rao KV, Kumar VSS, Tambur P (2017) A facile biosynthesis of copper nanoparticles: a micro-structural and antibacterial activity investigation. J Saudi Chem Soc 21:180–185